



Article

Evaluation of Fissures and Cracks in Bridges by Applying Digital Image Capture Techniques Using an Unmanned Aerial Vehicle

Eric Forcael ^{1,*}, Oswal Román ², Hayan Stuardo ², Rodrigo F. Herrera ³ and Jaime Soto-Muñoz ⁴¹ College of Engineering, Architecture, and Design, Universidad San Sebastián, Concepción 4081339, Chile² College of Engineering, Universidad del Bío-Bío, Concepción 4051381, Chile³ School of Civil Engineering, Pontificia Universidad Católica de Valparaíso, Valparaíso 2340025, Chile; rodrigo.herrera@pucv.cl⁴ College of Architecture, Construction and Design, Universidad del Bío-Bío, Concepción 4051381, Chile; jaimesito@ubiobio.cl

* Correspondence: eric.forcael@uss.cl; Tel.: +56-41-2487900

Abstract: The evaluation of cracks and fissures in bridge structures is essential to ensure the long-term safety, durability, and functionality of these infrastructures. In this sense, processing grayscale images and adjusting brightness and contrast levels can improve the visibility of cracks and fissures in bridge structures. These techniques, complemented by professional expertise and efficient inspection tools such as Unmanned Aerial Vehicles (UAVs), allow for a comprehensive and accurate structural integrity assessment. This study used the edge detection technique to analyze photographs obtained with a low-cost UAV as a means of image capture. This tool was used to reach hard-to-reach areas where there could be damage, thus making it easier to detect fissures or cracks. To capture the failures, two case studies, a small bridge and a large bridge, were selected, both located in Concepción City in southern Chile. During both inspections, cracks were detected that could affect the structure of the bridges in the future. To analyze these findings, ImageJ software 1.54h was used, which allowed the length and thickness of the cracks to be measured and evaluated. In addition, to validate the procedure proposed, real values manually measured on-site were compared with those delivered by the software analyses, where no statistically significant differences were found. With the method presented in this study, it was possible to quantify the damage, following the bridge maintenance standards established by the Ministry of Public Works of Chile, whose inspection criteria can be applied to other projects worldwide.

Keywords: bridge; fissures; cracks; grayscale-based image processing; edge detection; Unmanned Aerial Vehicle



Citation: Forcael, E.; Román, O.; Stuardo, H.; Herrera, R.F.; Soto-Muñoz, J. Evaluation of Fissures and Cracks in Bridges by Applying Digital Image Capture Techniques Using an Unmanned Aerial Vehicle. *Drones* **2024**, *8*, 8. <https://doi.org/10.3390/drones8010008>

Academic Editor: Higinio González Jorge

Received: 11 November 2023

Revised: 18 December 2023

Accepted: 27 December 2023

Published: 30 December 2023



Copyright: © 2023 by the authors. Licensee MDPI, Basel, Switzerland. This article is an open access article distributed under the terms and conditions of the Creative Commons Attribution (CC BY) license (<https://creativecommons.org/licenses/by/4.0/>).

1. Introduction

Maintenance can be defined as the necessary set of operations and works so that a construction site maintains the functional, resistant, and even aesthetic characteristics for which it was designed and built [1]. This process is divided into three stages: inspection, evaluation, and maintenance. The inspection stage consists of information collection, visual detection of the damage, and contrast of what is observed regarding technical references. The inspection methodology that is currently used contemplates the use of different means of transport to reach places of difficult access, such as trucks with inspection platforms, reticulated cabins, and even equipped hanging workers when necessary.

In this sense, it is important to emphasize that although the use of aerial vehicles has been decreasing in some industries, UAV technologies continue to bring positive impacts on the government's responsibilities in terms of infrastructure management, especially in bridges whose serviceability and reliability are declining and consequently jeopardize public safety [2]. From this perspective, government agencies in all countries can take advantage of drones to perform regular inspections of bridges, providing up-to-date data

for informed decisions and facilitating proactive maintenance planning, rapid emergency response, risk management, and the development of transparent policies that promote citizen participation in monitoring and understanding the status of bridges structures.

Among the damages detected in bridges are fissures and cracks, where thickness is the most important indicator in bridge maintenance; therefore, it is necessary to quantify it accurately [3]. Thickness is a determining factor since it defines the engineering threshold between a fissure and a crack, which is 5 mm according to the criteria of the Chilean Ministry of Public Works in its deterioration catalog [4]. To quantify the thickness accurately, a card containing a thickness ruler in millimeters is used, which utilization demands to be very close to the inspected element [5]. The evaluation stage requires the participation of specialized engineers, who will define the causes of the fissures/cracks and issue the technical specifications for their repair [4]. Finally, in the maintenance stage, the maintenance team gets ready to repair the damage based on the specifications provided by the specialists.

In addition, concrete structures under seismic loading consider stress cracking, confinement effect in compression, and cyclic behavior. Constitutive laws of damage mechanics are usually based on damage variables to describe the axial behavior of concrete in tension and compression. These variables act as the memory of the material, being able to record accumulated irreversible damage from which it cannot be recovered [6], where difficulties in evaluating cracks and fissures in bridge structures are found. Jeong et al. [7] state that one of the most difficult damages to quantify are cracks, especially under the deck and in the beams, because these elements are located in places that are difficult to access. The difficulty of taking measurements increases directly with the structural complexity of the bridge, especially if its location is in inhospitable places where access by traditional means is not possible, among other factors. Even though the current solutions partially solve the access problem, they bring with them adverse effects; for example, the case of the inspection truck brings issues of traffic cut-off for one of the bridge lanes, generating increased vehicular congestion while the inspection work is being carried out, lasting even several hours. Another scenario is the use of equipped hanging workers, which puts those inspecting under these conditions at risk, making the inspection process more time-consuming and dangerous. In summary, the current alternatives bring increased operating costs, adverse effects, and, depending on the bridge, long inspection times.

On the other hand, the advent of the Construction 4.0 concept in the last decade has brought about a change in the perspective of inspection work, including technologies that increase efficiency, innovation, and productivity. One of the technologies that make up the Construction 4.0 concept is robotics [8]. Currently, robotics is being used to inspect bridges [9] through Unmanned Aerial Vehicles (UAVs) that make aerial coordination, monitoring, and real-time inspection possible. Similarly, diverse research has been conducted on the use of UAVs in the construction and infrastructure ambits, such as progress monitoring, condition inspections, and safety inspections [10]. In this sense, the ability to capture high-quality audiovisual material, complemented with damage analysis methods, makes UAV a good alternative to access difficult-to-reach places, achieving to record damage through images in a short time.

The inspection results are images that must be processed to improve their quality and identify the damage they contain. For this task, there are grayscale-based techniques focused on enhancing the visibility of the image by highlighting fissures through a modification of brightness and contrast [7]. In general terms, these procedures utilize RGB images that—after applying some filtering techniques—allow the extraction of new images in gray tones whose grey-level graphs provide information. On the other hand, to define the contour of the damage, there is an edge detection technique that uses algorithms in MATLAB or Python programming language. This technique is characterized by detecting abrupt changes in image intensity and highlighting them [11]. In this research, the use of UAVs as a means of transport and visual information channel combined with image

processing was considered a good alternative for the evaluation of cracks and fissures in bridges.

To evaluate the techniques mentioned above, two case studies were analyzed: a small bridge called “Estero Nonguén Bridge” and a large bridge named “Llacolén Bridge”, both located in Concepción City in southern Chile. The visual inspections were performed with an unmanned aerial vehicle (UAV), model DJI Mavic 2 Pro. In addition, the ImageJ software was used for image processing, which contained tools for enhancement using grayscale and edge detection. Also, image scaling and measurement procedures were considered based on a pixel-by-pixel basis.

With the measurements, the damages of both bridges were described and classified in terms of whether they corresponded to fissures or cracks or whether they produced an effect structurally, and consequently to define their severity according to the Chilean Ministry of Public Works criteria [4], in addition to determining the possible causes of failure based on a study of cracks conducted in other researches [12]. With the thickness measurements along the failure (either a crack or a fissure), the average and maximum thickness were identified, in addition to constructing Length vs. Thickness graphs to analyze the behavior of each failure.

Thus, the main aim of this research is to evaluate cracks and fissures in bridges by applying grayscale techniques and edge detection using UAVs. On the other hand, the objectives can be classified as (a) to characterize the behavior of a UAV as a bridge inspection tool concerning the current legal standards, environmental factors, and the scenario surrounding each bridge to identify limitations in the operability of these aircraft; (b) to apply grayscale and edge detection techniques for image processing to improve the visibility and definition of the edges that enclose the cracks and fissures found through visual inspections on bridges; (c) to identify the damage level of cracks and fissures along with detailed analyses about their characteristics.

2. Literature Review

2.1. Structural Incidence and Severity of Cracks and Fissures

The severity scale considers minimum, medium, high, and very high categories. The severity assignment will depend on the structural incidence of the damage and its thickness; the greater the opening, the higher the severity. Table 1 shows the structural incidence of fissures (opening less than 5 mm), considering the cause of damage within the bridge with their general thickness ranges. In the case of cracks, the same classification is used, with the difference that their opening is greater than 5 mm.

Table 1. Classification of cracks and fissures according to their impact on bridge structural behavior (adapted from [4]).

Fissures (<5 mm) and Cracks (>5 mm)—Do They Affect Structural Behavior?			
Yes	Range	No	Range
At 45° in the web of beams or slabs, next to supports, or due to stresses (compression, bending, or shear)	<0.7 mm	Due to the settlement of the side wall of an abutment	>0.7 mm
Due to incorrect dimensioning of the element	>0.7 mm	Due to a lack of coating	<0.7 mm
Due to the pushing of one element on another	>0.7 mm	Due to hydraulic shrinkage	<0.7 mm

Note: Range columns only apply in the case of fissures. The thickness of the cracks is greater than 5 mm.

It has to be mentioned that failures that also affect structural performance include those caused by corrosion of reinforcements, freeze–thaw cycles, and poor construction workmanship.

2.2. Crack Analysis in Structures

Some researchers have investigated cracks and fissures in concrete structures [12]. Cracks caused by compressive, flexural, or shear stresses are among the most relevant due

to their structural incidence. They should be constantly inspected to identify when they appear and take measures on time. This type of failure can be classified as (a) cracks in a plastic state (caused by errors in construction methods or by a deficiency in the control of water supplied to the concrete), (b) cracks in a hardened state (caused by volumetric changes due to temperature and humidity or by oxidation of the reinforcing steel), (c) stress-induced failures (compression, bending, shear or deflection). These failures are expected to be inspected by UAVs instead of using traditional methods.

2.3. Photography within Damage Inspection

In the inspection stage, the most important type of information is imagery [13]. Photographs record the damage or environmental conditions in a structure, which can be analyzed as many times as necessary, zoomed in, or drawn lines. Therefore, they are very useful for identifying cracks or fissures in bridges, where a camera mounted on a drone allows for detailed damage identification in difficult-to-access places, for example, under the deck [14].

To capture a photograph that accurately records the damage in an inspection, the following factors must be considered:

- (a) Image resolution: it depends on the resolution of the camera used. The higher the resolution, the greater the number of pixels, allowing a much better breakdown of its content. However, it is important to emphasize that not only the resolution or the high number of pixels are the relevant factors exclusively, but also the quality of the camera, the size of the sensor (better APS-C or full frame formats), and indeed the sensor resolution.
- (b) Light presence: to detect damage, the inspection must be carried out with the necessary amount of light since the perception of a camera is not the same as that of the human eye, where the acquired light provides unique photographic capabilities, such as the ability to digitally refocus the scene after exposure, extend the depth of field, and alter the viewpoint and perspective [15].
- (c) Camera-element distance: it defines the scale ratio in the image. The scale corresponds to the number of pixels in a unit of length (m, cm, mm, etc.). In scientific photography, one of the ways to define the scale is based on the known measurement within the image [16], which can be obtained from plans, inspection sheets, or other similar sources.
- (d) Camera angle: the distortion of measurements is not only determined by the camera angle but is also characterized by the radial and tangential distortion coefficients, which define the distortion model of a camera.

Figure 1 shows the perspective distortion effect caused by camera position and how it affects the perception of the actual measurements [14,16]. For this reason, photographs aligned to the damage are required to decrease the perspective distortion effect.

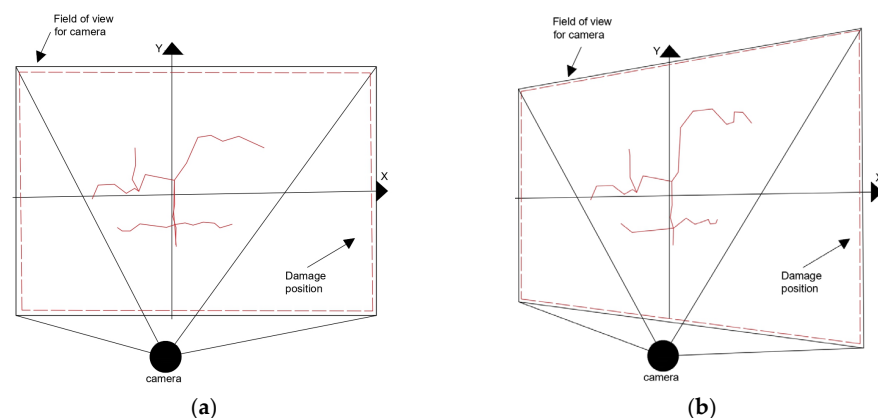


Figure 1. Perspective distortion effect. (a) Camera aligned with the defect, (b) a camera placed at the side of the damage (Adapted from Seo et al. [14]).

It is important to note that when there is an image with perspective distortion, scale variations can be observed. Therefore, to avoid these perspective distortions, when taking a photograph, the drone has to be positioned perpendicularly in front of the element to be inspected. In this sense, one of the strengths of using drones in the inspection of remote places (e.g., under a bridge in the middle of a river) is the versatility of this type of equipment to reach these difficult-to-access places and, in this case, capture photographs by positioning it completely orthogonal to the inspected element. However, there will always be some exceptions where the drone cannot be located perpendicularly to the observed element, in which case the use of photogrammetric processing can be a very valuable tool to correct this problem.

2.4. Techniques to Improve the Quality of a Grayscale Image

When collecting images, some techniques related to grayscale use and edge detection have to be considered, which are briefly summarized below.

Grayscale

The purpose of this technique is to convert color images to gray tones to adjust their contrast [14]. In this sense, according to Jeong et al. [7], there are three ways to improve the visibility of an image: (a) Image Intensity Adjustment, which allows for extending the range of tones to the extremes to contrast those areas with an excess of gray; (b) Equalized Histogram, which modifies the intensity values to achieve a tone histogram similar to the uniformly distributed histogram or other user-specified distribution, and (c) Adaptive Equalized Histogram—a mixture of the previous two techniques, which can be applied to small regions of the image defined as mosaics, by improving the quality of each mosaic and combining them through bilinear interpolation to eliminate artificially induced boundaries.

2.5. Edge Detection Technique

This technique uses grayscale conversion to detect and highlight sharp intensity changes in the image [11]. It is based on mathematical sciences using convolution kernels composed of matrices to generate vertical and horizontal derivatives of a function $f(x)$, where the first derivative allows finding the maximum and minimum points, and the second derivative finds the points where the functions become zero [17,18]. Edge detection algorithms are divided into Gradient-based and Laplacian methods [19,20], where to detect edges, the first one uses the first derivative, while the Laplacian method uses the second derivative [21]. Figure 2 shows the edge changes identified in an image converted to grayscale with the first and second derivatives.

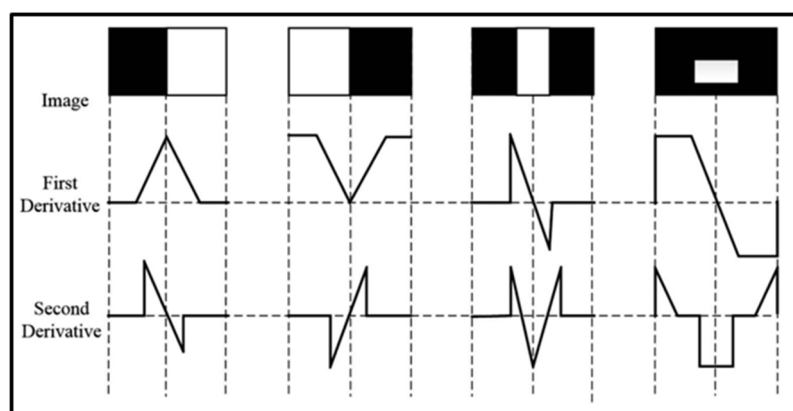


Figure 2. Detection of edge changes with first and second derivatives (adapted from Lei et al. [21]).

3. Research Method

This research aimed to evaluate the grayscale enhancement techniques and the edge detection technique in the images captured by a UAV. To achieve this objective, the fol-

lowing research method was used, which was divided into three stages: (1) case studies, (2) UAV selection and flying, and (3) analysis and results.

3.1. Stage 1: Case Studies

Both bridges are located in Concepción City in southern Chile. The first corresponds to a small bridge with a single span of 20 m. The second one is a large bridge, 2157 m in length. These bridges were selected because their physical characteristics represent two extremes of interest in their structural complexity, size, and traffic demand to which they are subjected daily.

3.2. Stage 2: UAV Selection and Flying

After evaluating diverse UAVs, the UAV selected was a Mavic 2 Pro model of the DJI line, frequently used because of its low cost, which has a built-in camera with a resolution of 5472×3648 pixels, with a focal length of 28 mm and a shutter time of $1/8000$ s. With this equipment, the bridge inspection was carried out, capturing the damages and defects with well-defined images. Before the inspection, a flight path was drawn, considering the elements of each bridge and the existing obstacles. The flight time was evaluated based on battery duration (31 min). It should also be mentioned that the flight was carried out manually, based on the flight route planned according to the terrain conditions.

3.3. Stage 3: Analysis and Results

After completing the inspection and taking the photographic record, the images were downloaded from the aircraft's memory card. The photographs selected for each case study were analyzed in ImageJ software [11]. This open-source software for processing and analyzing scientific images was used in Version 1.53t. Its Java source code is freely available, and in the public domain, no license is required. With the line tool, pixel-based measurements of the thickness and length of the faults were taken.

Once the images were processed in the ImageJ software, the fissures and cracks were delimited manually to differentiate them from other lines that exist within the image. To do so, fissures and cracks were defined, creating paths that exceeded the image, using the zoom and rule tools that the program has. In terms of dimensions, to measure the fissures and cracks (in millimeters), a known measure within the image was used as a pattern, for example, any known dimension of some structural element (coming from the structural drawings), such as the height of a beam or the width of a column, and based on this information then scale the complete image and thus obtain precise measures of fissures and cracks. Consequently, Figure 3 describes graphically how these measurements were taken after edge detection was applied to the image. The maximum thickness defined whether the damage corresponded to a crack or a fissure, its structural incidence, the possible cause of the damage, and its severity.

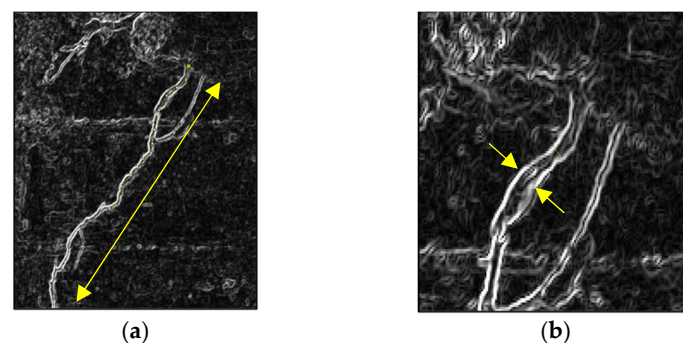


Figure 3. Measurements taken with ImageJ. (a) Yellow line shows the length of the crack or fissure, (b) Yellow lines show the width of the crack or fissure.

In summary, Figure 4 shows a flow diagram of the methodology used to acquire the information needed to evaluate the fissures and cracks in bridges by applying digital image capture techniques with a UAV.

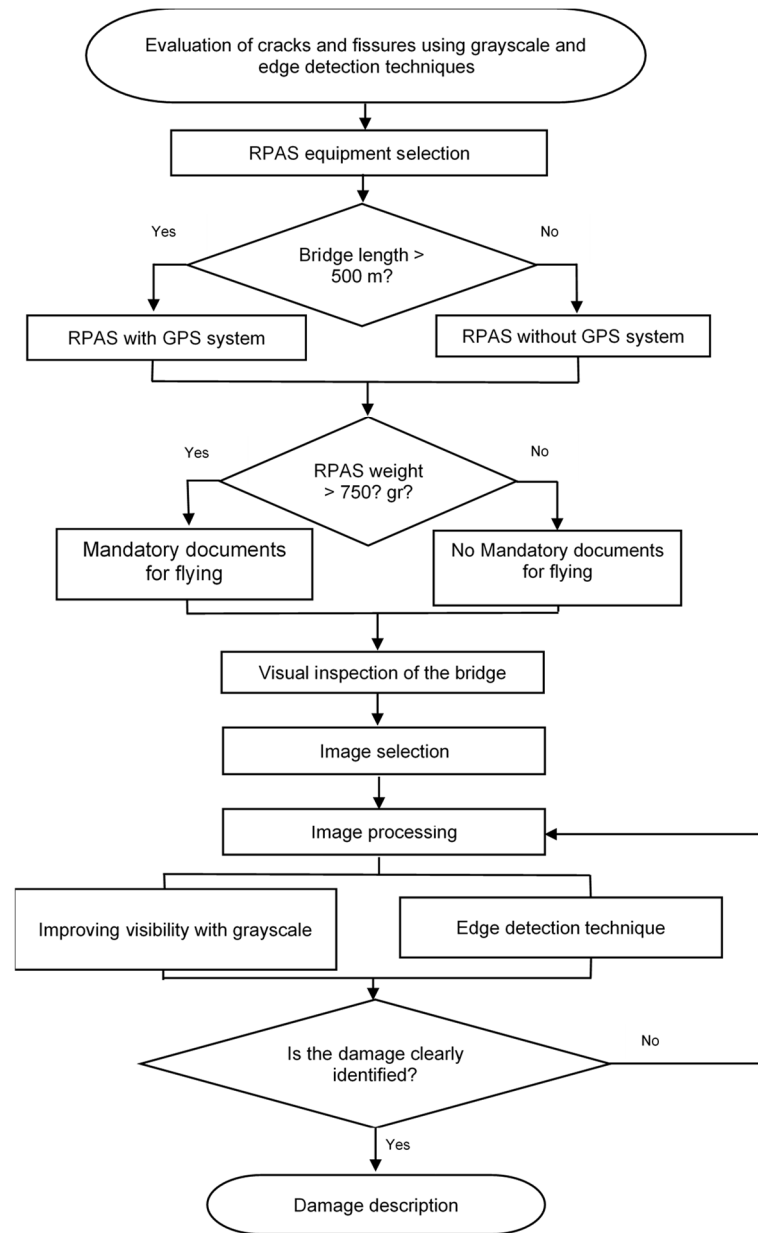


Figure 4. Flow diagram with the methodology used in this research.

4. Analysis and Results

4.1. Case 1: Estero Nonguén Bridge (Small Bridge)

4.1.1. General Description

It has a length of 20 m and a roadway width of 7 m. The deck has a roadway formed by a reinforced concrete slab with one lane in each direction and two 1.5 m wide pedestrian walkways. It has two abutments and, in the middle, a stock wall with a span width of approximately 8 m.

4.1.2. Flight Route

The flight route is detailed in Figure 5, consisting of a flight over the roadway starting at the side of the bridge. The flight started upstream and flew over the bridge in a downstream

direction, where the UAV was introduced in both spans to return to the starting point upstream of the bridge. The height of the deck allowed the aircraft to stay stable during the flight and away from the estuary channel. As the inspection progressed, some complexities were encountered. In one of the spans, plant material was found obstructing the passage, as well as facility cables and a pipe that crossed the stream at the height of the deck.

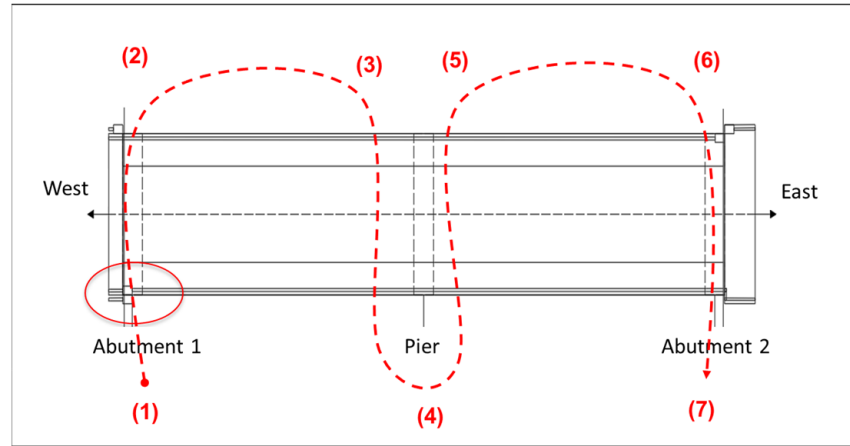


Figure 5. Small bridge damage inspection flight path (the dash line shows the flight path of the drone, the numbers show the corresponding changes in the direction where the photographs were taken, and the red circle shows the exact location to be analyzed for cracks or fissures).

4.1.3. Photographic Record and Image Selection

The entire structure was inspected with a full battery charge in an estimated time of 30 min, obtaining a total of 45 photographs. Figure 6 is a sketch of the bridge identifying the location of the potential cracks.

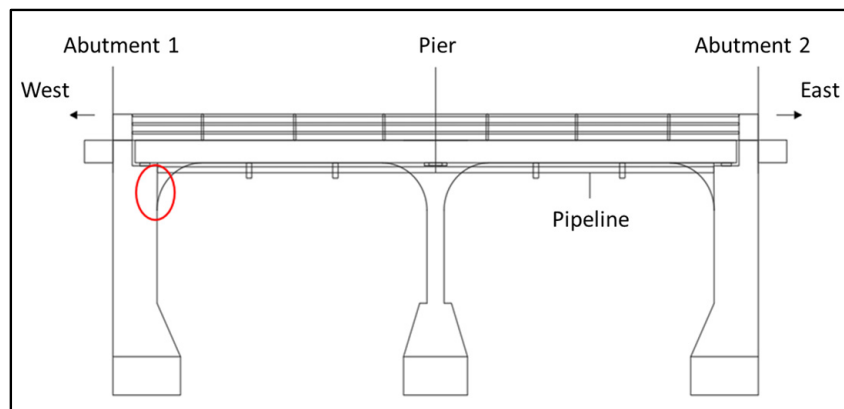


Figure 6. Location in elevation of the analyzed crack in the small bridge (the red circle shows the exact location to be analyzed for cracks or fissures).

4.1.4. Image Calibration

A crack at abutment 1 of the bridge originated from the junction with a steel pipe that crosses the estuary was identified, which failure (crack or fissure) is shown in Figure 7. As only one failure was found, it was assigned with the number 1.1 (Figure 7). The measurement of the wing wall's top was used, corresponding to 20 cm, as shown in Figure 7. Within the photograph, 20 cm was equivalent to 272 pixels, resulting in a scale of 1.36 pixels/mm.



Figure 7. Identification of Crack 1.1 at the small bridge.

4.1.5. Grayscale Application

The image quality was improved by modifying the brightness and contrast levels in ImageJ by applying the grayscale tool. Figure 8 shows the process that was carried out on the image. In (a) and (b), the image is shown with grayscale applied with its respective gray histogram, where the brightness and contrast have not yet been modified. Then, in (c) and (d), the image is shown with the adjusted brightness and contrast.

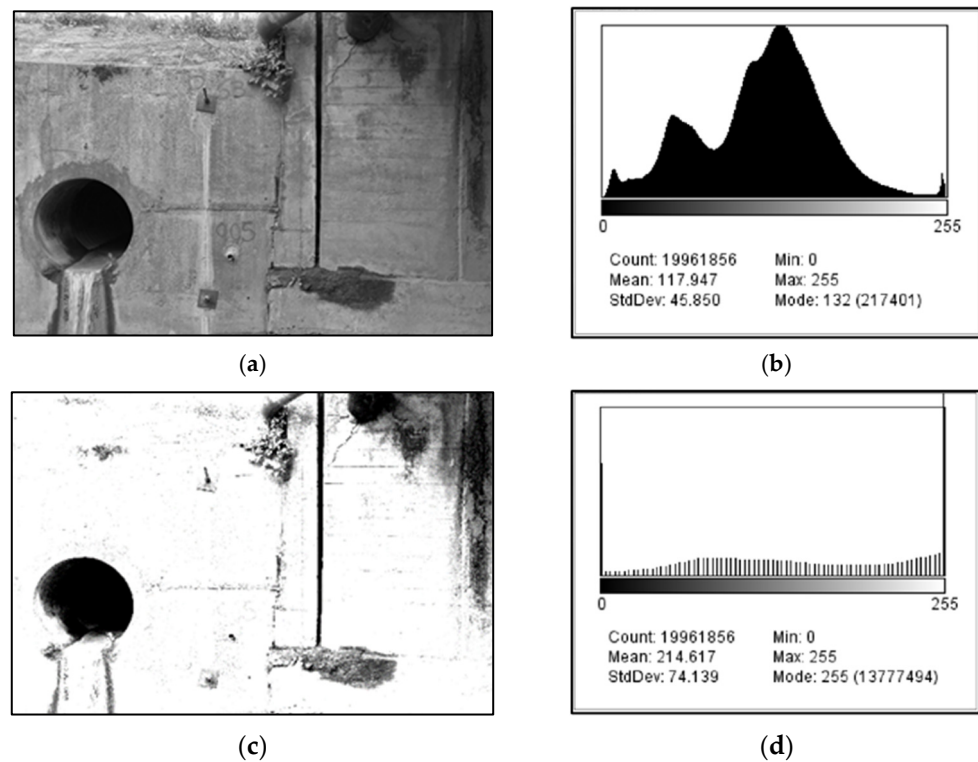


Figure 8. Image Crack 1.1 of the small bridge processed with ImageJ. (a) Grayscale application, (b) Grayscale histogram, (c) Image quality enhancement, (d) Enhanced image histogram.

4.1.6. Application of Edge Detection Tool and Damage Description

The edge detection tool’s effect on this image was appropriate since it mostly defined the limits of the crack concerning the reinforced concrete wall in which it was contained. Figure 9 shows the application of this tool; (a) and (b) show the edges of the damage and the crack highlighted with white pixels, and the areas without defects are complete with black, which is why most of the pixels are at the extremes in the histogram. Thus, it was possible to highlight the crack to perform measurements guided by the detected edge.

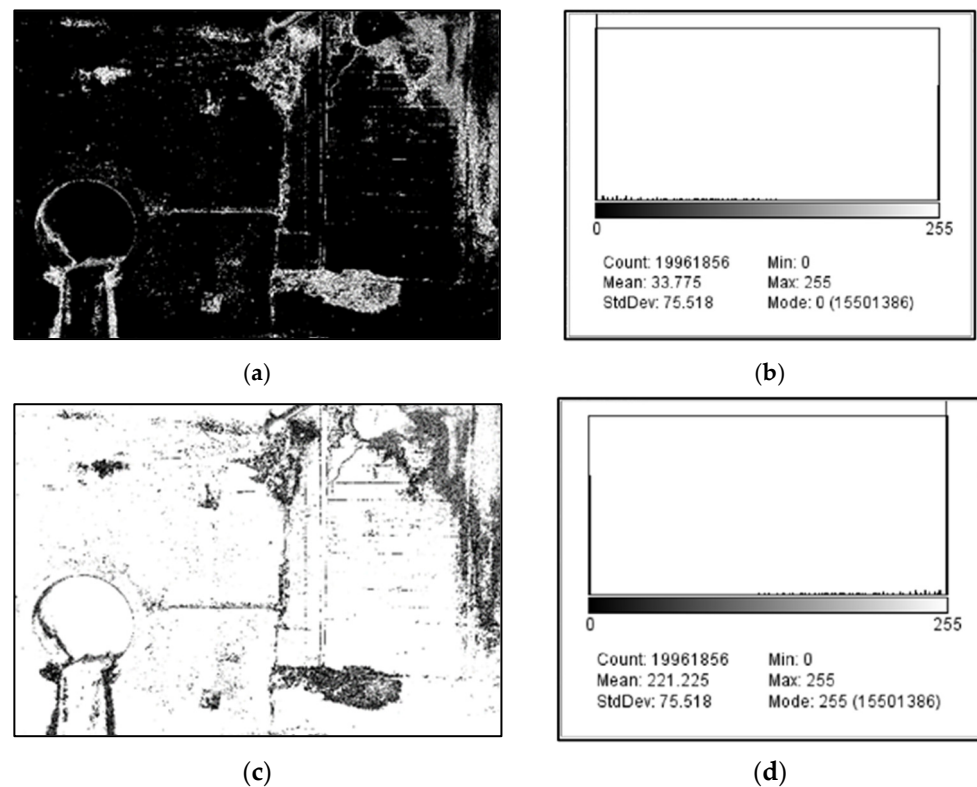


Figure 9. Crack image 1.1 of the small bridge analyzed with ImageJ. (a) Application “find edges”, (b) Histogram image with “find edges” applied (c) Application “invert” grayscale, (d) Histogram of the image with “invert” applied.

In (c) and (d), the “invert” tool was applied to invert the histogram by changing the pixels from black to white, standing out the crack. Having both images where the crack could be seen without problems, the image from (c) was used to measure the thickness and length of the crack.

Measurements were taken along the failure to obtain its length, maximum, and average thickness. With the maximum thickness, the failure was defined as a crack or fissure. Accordingly, Table 2 summarizes the description of the crack.

Table 2. Damage description of the crack 1.1 in the small bridge.

N°	Location (Element)	Length (cm)	Maximum Thickness (mm)	Average Thickness (mm)	Damage	Does It Affect Structurally?	Possible Cause	Estimated Severity
1.1	Abutment 1	54.04	6.401	7.79	Crack	Yes	Shear stress	Low

4.1.7. Length vs. Thickness Graph

The results of the measurements along the crack are shown in Figure 10. Measurements started from the crack origin at the upper right end and progressed to the crack end at the lower left end. A total of 257 measurements were taken at a distance of approximately 2.1 mm each.

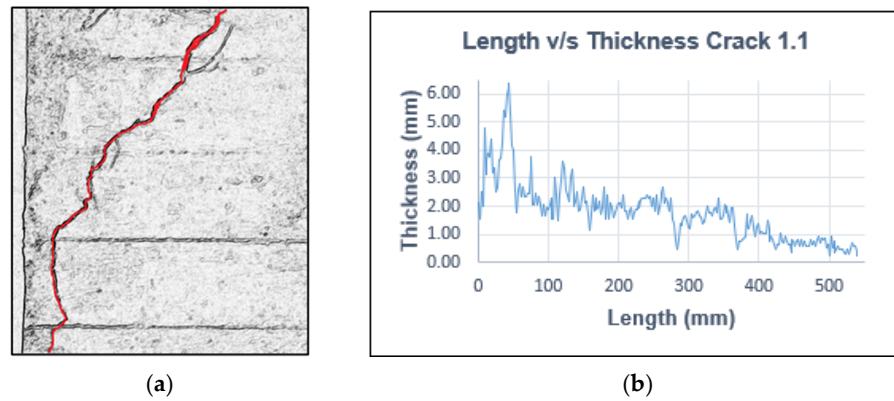


Figure 10. (a) Representation of crack 1.1 as seen in ImageJ (red line); (b) Thickness vs. Length graph of crack 1.1.

4.2. Case 2: Llacolén Bridge (Large Bridge)

4.2.1. General Description

This large bridge is divided into two sectors, one directly over the Bío-Bío River of 1782 m and a second sector outside the river of 375 m. The two bridge abutments are founded on 317 concrete piles of 1.5 m in diameter and variable lengths of 16 and 29 m. The piers are formed by 10 piles each except for the off-river extension at the north end, which is formed by six piles, and the off-river section that connects with an important avenue. Its deck has an 8 m dual carriageway with two lanes in each direction and two pedestrian walkways.

4.2.2. Flight Route

Due to the large size of this structure and dense traffic, only the northern sector of the bridge, covering four piers, was inspected. The flight path detailed in Figure 11 was traced starting at Pier 2 and proceeding to Pier 4, where each span was inspected until arriving at Pier 1, where the elevations were inspected too.

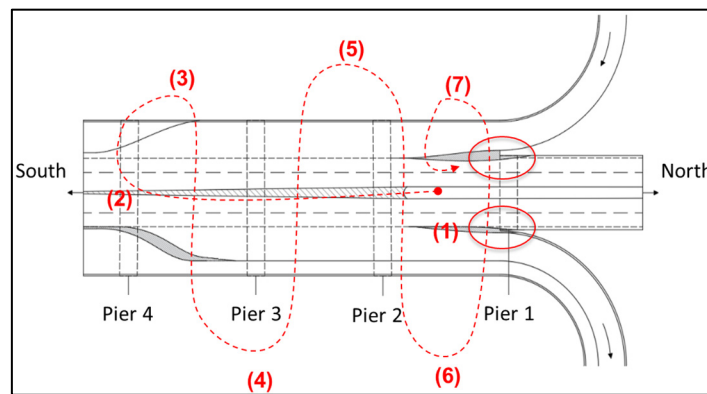


Figure 11. Large bridge damage inspection flight path (the dash line shows the flight path of the drone, the numbers show the corresponding changes in the direction where the photographs were taken, and the red circle shows the exact location to be analyzed for cracks or fissures).

During the inspection, some complexities were faced. The river flow caused difficulty in maneuvering the UAV, making it hard to keep a line of sight with the equipment, where, for some routes, the pilot was only guided by the camera. The dense traffic did not allow inspecting near or under the board in the area of a level crossing, and the presence of birds flying very close to the aircraft increased the risk of an accident.

4.2.3. Photographic Record and Image Selection

A full charge of the batteries was used to inspect the four piers of the bridge in approximately 30 min, taking 38 photographs. To analyze the identified cracks, the images shown in Figure 12 were selected. In section (a), the east view containing the crack network is shown, and in section (b), the west view containing a crack is shown. On the other hand, Figure 13 schematically shows the damage analyzed in ImageJ at the large bridge.

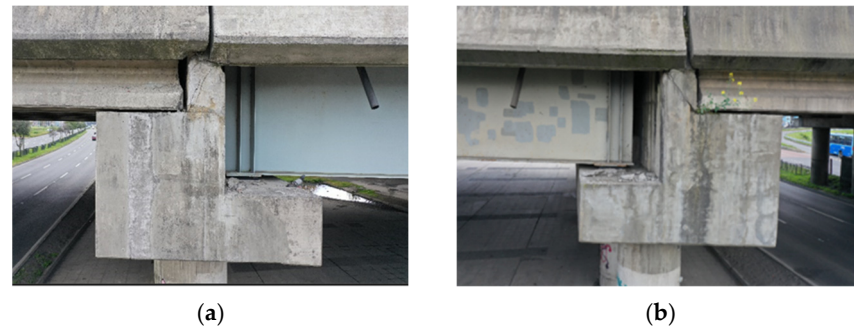


Figure 12. Images selected for crack analysis in the large bridge: (a) Header east view, (b) Header west view.

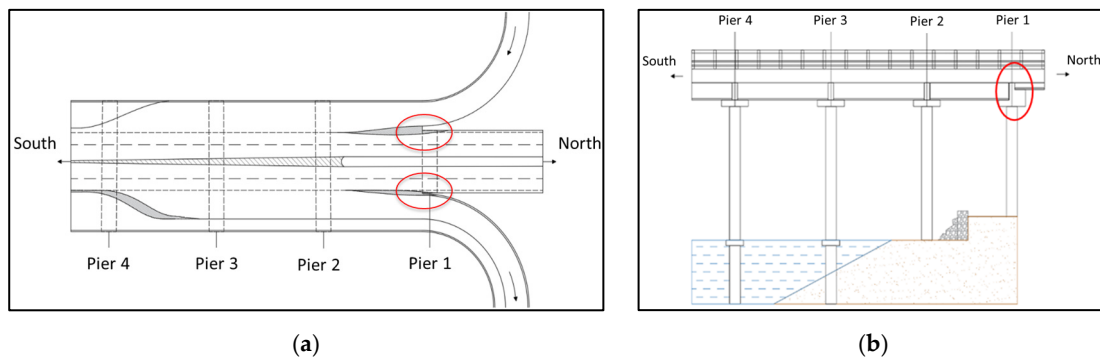


Figure 13. Inspected sector on the large bridge (Pier 1). (a) Plan view; (b) Elevation view (the red circles show the exact location to be analyzed for cracks or fissures).

4.2.4. Crack Numbering and Image Calibration

The crack numbering for the header east view was 1.1, 1.2, 1.3, 1.4, and 1.5, while for the header west view, it was 2.1, as shown in Figure 14.



Figure 14. Cracks resulting from shear stress in the head of pier 1. (a) East view, (b) West view.

4.2.5. Grayscale Application

Figures 15 and 16 show how the grayscale histogram was modified to highlight the cracks in the east and west elevations of the header.

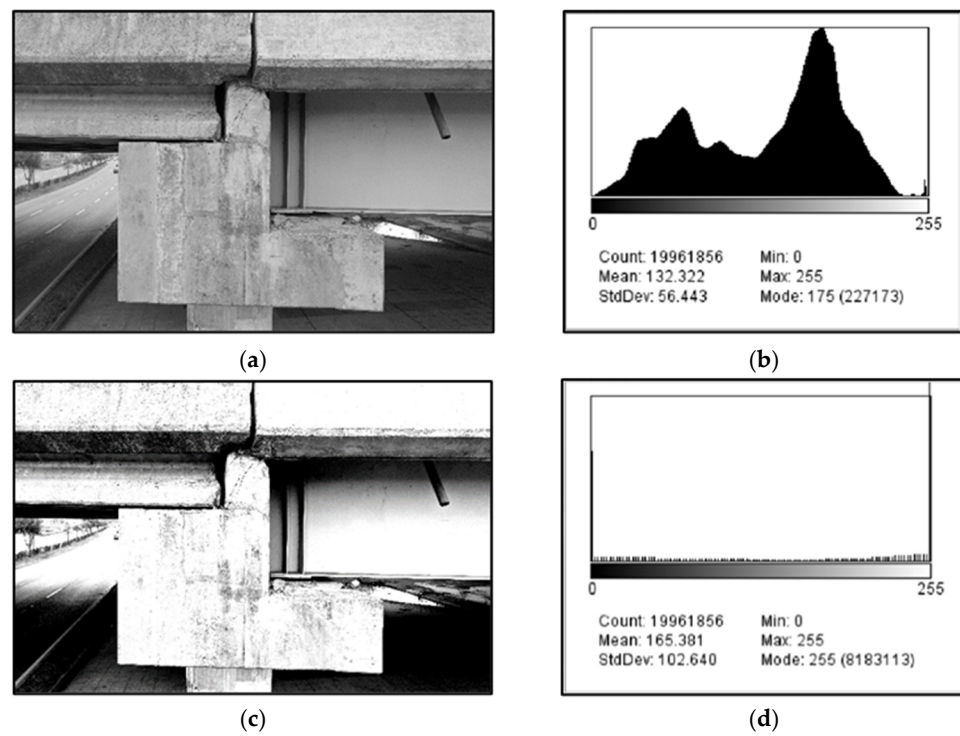


Figure 15. Crack Network Analysis in the large bridge header east view with ImageJ. (a) Grayscale Application, (b) Grayscale Histogram, (c) Image Quality Improvement, (d) Histogram Enhanced Image.

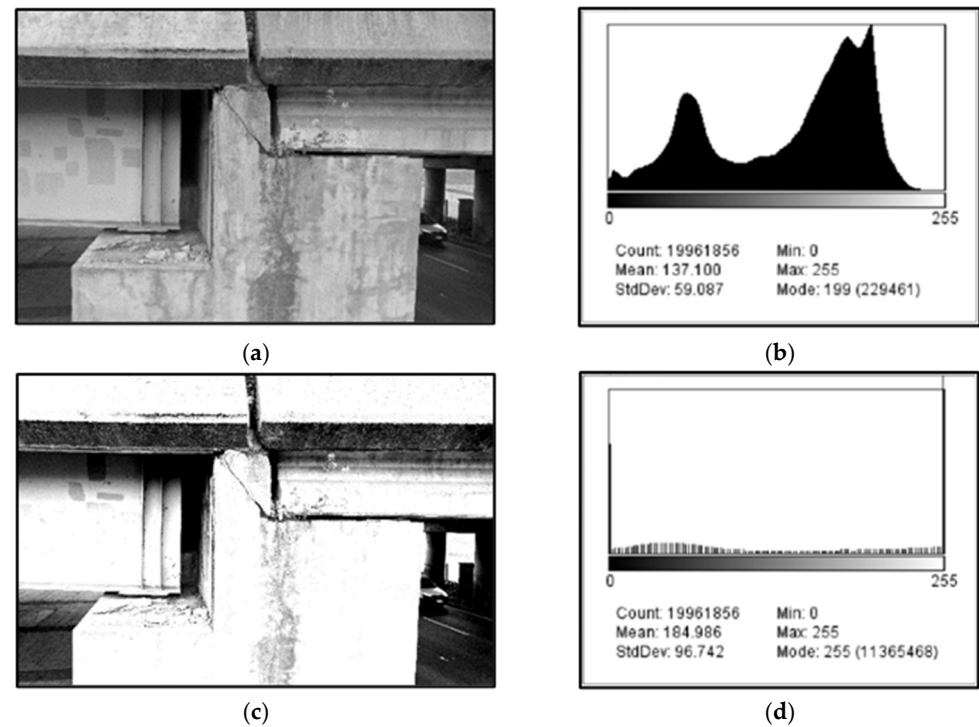


Figure 16. Crack Network Analysis in the large bridge header west view with ImageJ. (a) Grayscale Application, (b) Grayscale Histogram, (c) Image Quality Enhancement, (d) Enhanced Image Histogram.

4.2.6. Application of Edge Detection Tool and Damage Description

Cracks were located in the headers of Pier 1. The header in the eastern sector has a network of cracks that was divided into five cracks for individual analysis. The head in the western sector has only one crack.

Edge detection was applied to each image, obtaining different results. Figure 17 shows that this tool does not provide a good view of the crack network; rather, the trace is lost with the marks of the concrete. An attempt was made to simultaneously modify the brightness and contrast using edge detection. Still, it was not possible to highlight the cracks in the expected way, so only the image obtained in Figure 16c was considered for the quantification of damage.

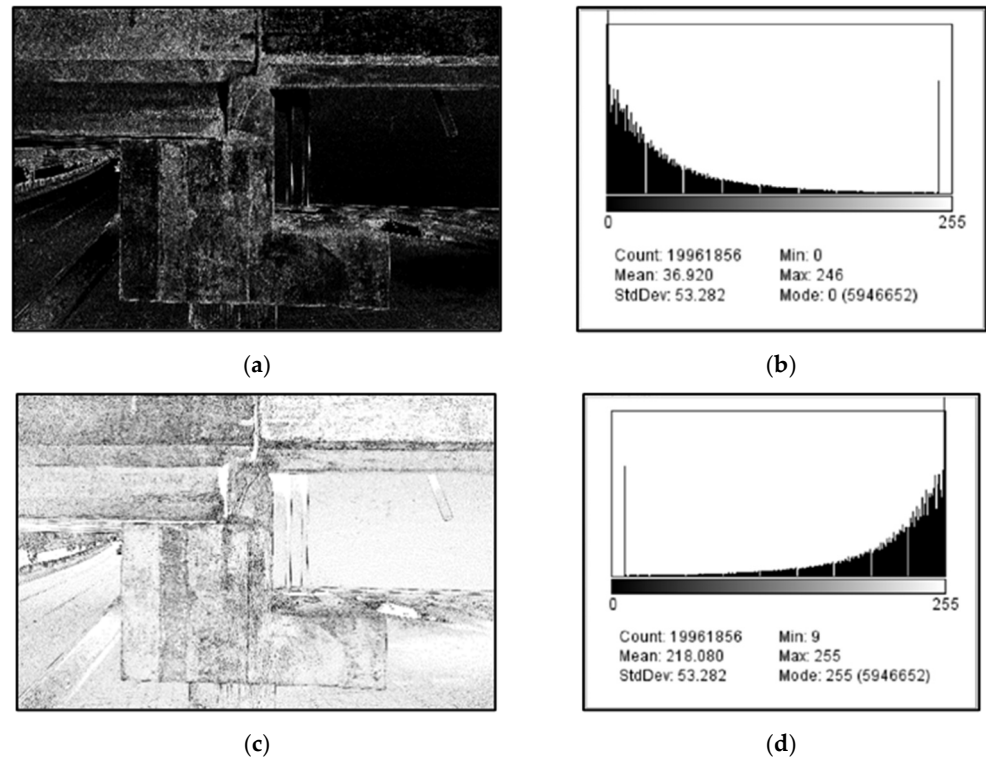


Figure 17. Crack Network Analysis in the large bridge header east view with ImageJ. (a) “find edges” application, (b) Histogram of the image with “find edges” applied, (c) Application of “invert” grayscale, (d) Histogram of the image with “invert” applied.

In the west view, a combination of brightness and contrast was obtained that positively supported the crack protrusion along with edge detection. As shown in Figure 18, the crack is visible in both (a) and (c) when the grayscale distribution is inverted. For this view, the image corresponding to Figure 18c was selected for damage quantification.

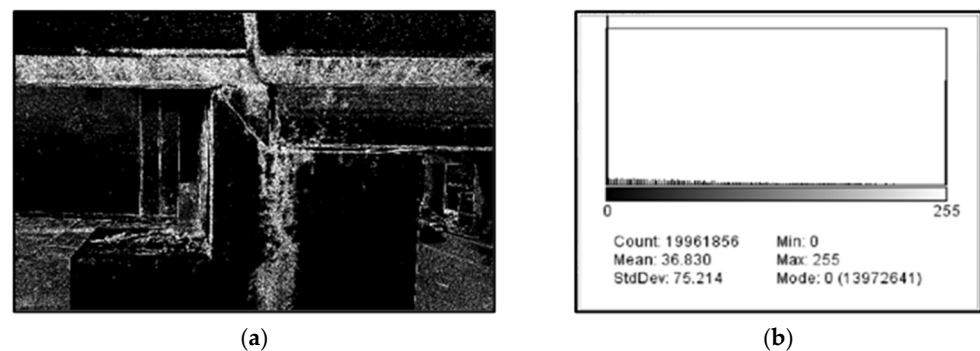


Figure 18. Cont.

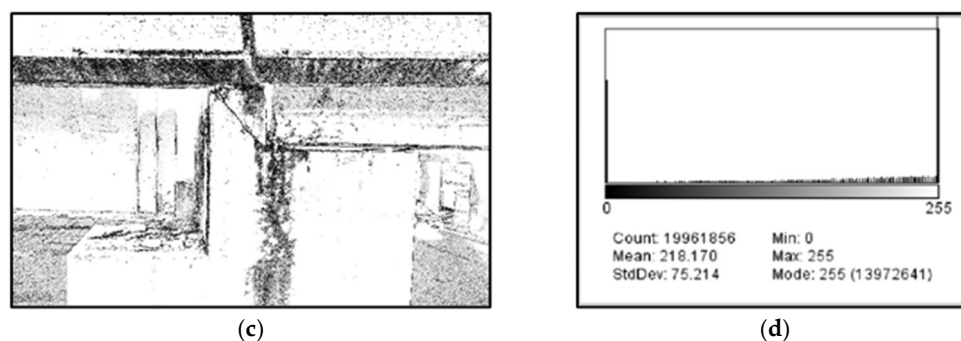


Figure 18. Crack Network Analysis in the large bridge header west view with ImageJ. (a) “find edges” application, (b) Histogram of the image with “find edges” applied, (c) Application of “invert” grayscale, (d) Histogram of the image with “invert” applied.

Measurements were taken along the lengths, maximum thicknesses, and averages. The maximum thickness showed that all the failures corresponded to cracks. Table 3 summarizes the description of the cracks of the large bridge based on the Ministry of Public Works bridge maintenance criteria.

Table 3. Damage description of the large bridge failures.

N°	Location (Element)	Length (cm)	Maximum Thickness (mm)	Average Thickness (mm)	Damage	Does It Affect Structurally?	Possible Cause	Estimated Severity
1.1	Header pier 1 East Sector	42.49	3.67	1.69	Fissure	Yes	Shear stress	High
1.2	Header pier 1 East Sector	53.23	4.28	0.89	Fissure	Yes	Shear stress	High
1.3	Header pier 1 East Sector	31.72	1.23	0.53	Fissure	Yes	Shear stress	High
1.4	Header pier 1 East Sector	30.11	0.99	0.47	Fissure	Yes	Shear stress	High
1.5	Header pier 1 East Sector	16.92	1.48	0.59	Fissure	Yes	Shear stress	High
2.1	Header pier 1 West Sector	52.3	4.1	1.7	Fissure	Yes	Shear stress	High

4.2.7. Length vs. Thickness Graph

The measurements obtained from ImageJ were exported to Excel to construct a “Length v/s Thickness” graph to analyze the behavior of the failures. The fissures turned out to have a little predictable behavior; the section losses produced the thickness in certain zones to be greater than the trend, causing the graphs to have an irregular behavior. Figures 19 and 20 show the graphs of the five fissures in the east view, and Figure 21 shows the graph of the fissures identified in the west view.

4.3. Validation of the Procedure Developed

According to Sarkar et al. [22], in crack detection and concrete property exploration, the recording process of large volumes of structural imagery demands significant time and effort, and the elaboration of these datasets can be financially onerous and require considerable human resources. Thus, because of the importance of saving time and resources, it is adequate to work with no more than 30 data since the Central Limit Theorem allows stating that a sampling distribution of sufficiently large size of samples ($n \geq 30$) will be normally distributed [23]. Despite the previous fact, as a confirmatory check, the Shapiro–Wilk test was run for the present study. Consequently, after applying the procedure developed in the two case studies, 30 new crack samples were randomly selected to validate the procedure,

which is shown in Table 4. The first column of data shows the theoretical measurements obtained from the ImageJ software, while the second column shows the field measurements using a crack width ruler. Based on the verification whether the differences between the theoretical and actual measurements followed a normal distribution, the statistical comparison test to use was defined.

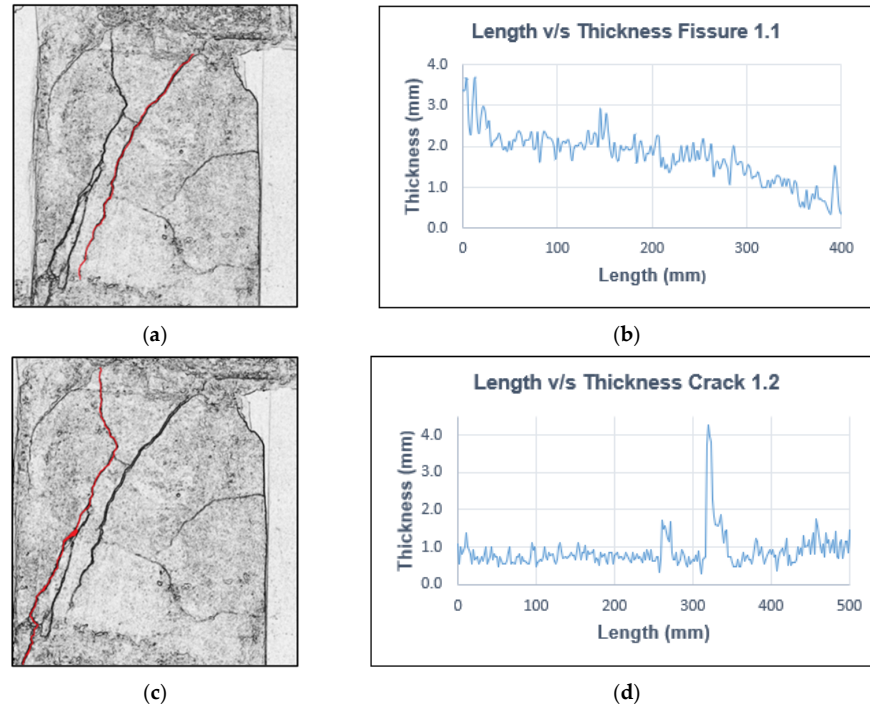


Figure 19. Crack Network Analysis east view of the large bridge. (a) Crack 1.1 Processed in ImageJ (red line); (b) Crack 1.1 Thickness v/s Length graph; (c) Crack 1.2 Processed in ImageJ (red line); (d) Crack 1.2 Thickness v/s Length graph.

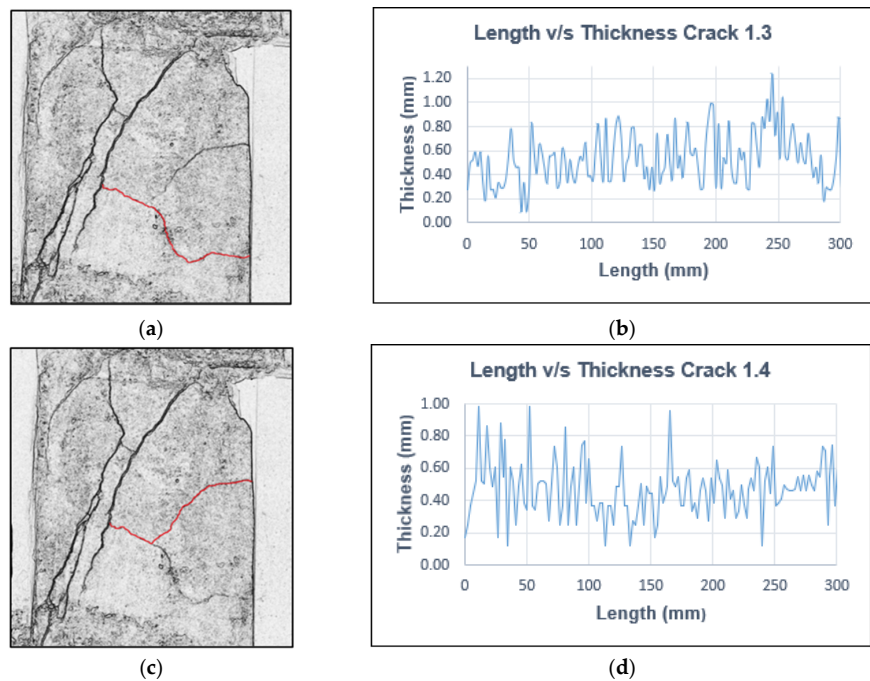


Figure 20. Cont.

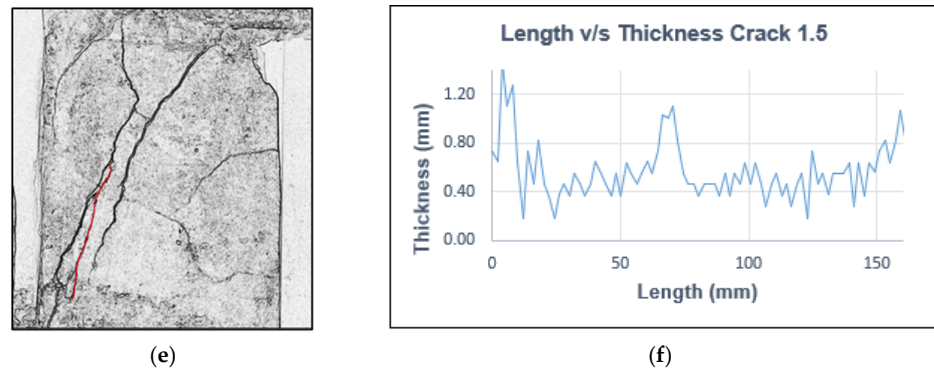


Figure 20. Crack Network Analysis east view of the large bridge. (a) Crack 1.3 Processed in ImageJ (red line); (b) Crack 1.3 Thickness v/s Length graph, (c) Crack 1.4 Processed in ImageJ (red line); (d) Crack 1.4 Thickness v/s Length graph; (e) Crack 1.5 Processed in ImageJ (red line); (f) Crack 1.5 Thickness v/s Length graph.

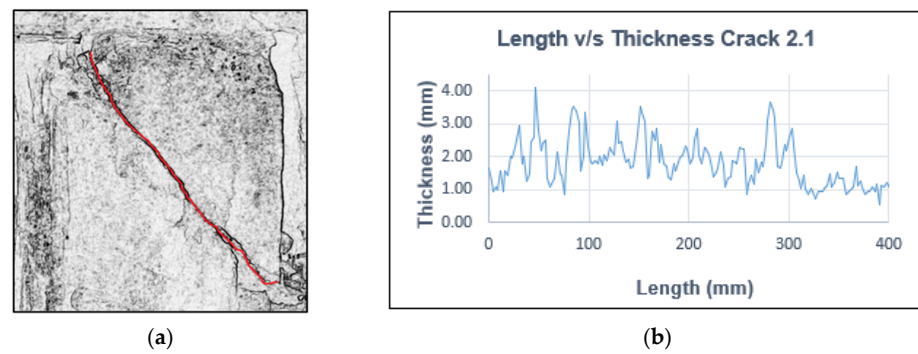


Figure 21. Analysis of Crack 2.1 of the large bridge west view (a) Crack 2.1 processed in ImageJ (red line); (b) Thickness v/s length graph of crack 2.1.

Table 4. Theoretical and real crack/fissures measurements.

Crack	Thickness (mm)		Difference (Theoretical–Actual)	Length (mm)		Difference (Theoretical–Actual)
	Theoretical	Actual		Theoretical	Actual	
1	3.053	3	0.053	331.032	330	1.032
2	1.973	2	−0.027	189.570	190	−0.430
3	2.993	3	−0.007	917.560	920	−2.440
4	1.949	2	−0.051	326.640	330	−3.360
5	1.017	1	0.017	201.318	200	1.318
6	1.984	2	−0.016	79.300	80	−0.700
7	3.139	3	0.139	940.600	920	20.600
8	2.015	2	0.015	758.000	730	28.400
9	2.982	3	−0.018	562.000	558	4.000
10	3.067	3	0.067	737.000	740	−3.000
11	3.984	4	−0.016	300.180	300	0.180
12	2.951	3	−0.049	232.340	230	2.340
13	3.892	4	−0.108	230.190	230	0.190
14	1.963	2	−0.037	277.900	280	−2.100
15	0.984	1	−0.016	448.500	450	−1.500
16	2.906	3	−0.094	121.500	120	1.500
17	1.033	1	0.033	360.700	360	0.700
18	2.012	2	0.012	995.700	1000	−4.300
19	0.984	1	−0.016	475.600	475	0.600
20	2.054	2	0.054	1211.800	1210	1.800
21	0.986	1	−0.014	453.900	450	3.900

Table 4. Cont.

Crack	Thickness (mm)		Difference (Theoretical–Actual)	Length (mm)		Difference (Theoretical–Actual)
	Theoretical	Actual		Theoretical	Actual	
22	1.033	1	0.033	145.600	145	0.600
23	4.911	5	−0.089	604.770	604	0.770
24	4.994	5	−0.006	711.220	711	0.220
25	4.872	5	−0.128	525.120	525	0.120
26	10.29	10	0.290	362.260	360	2.260
27	9.760	10	−0.240	2796.640	2800	−3.360
28	4.959	5	−0.041	1899.680	2000	−100.320
29	4.910	5	−0.090	233.980	240	−6.020
30	4.094	4	0.094	484.290	485	−0.710

After running the Shapiro–Wilk test, it was not possible to confirm the normality of the data [24,25]. Therefore, to verify if the measurements obtained by the ImageJ software can be assimilated into the real measurements obtained in the field, the non-parametric Wilcoxon test was used. This non-parametric statistical test is used to compare two related samples, matched or repeated measurements in a single sample to assess whether their population mean ranks differ [26], where the null hypothesis H_0 = the thicknesses and lengths of cracks and fissures obtained by the ImageJ software are equal to the real measurements obtained on-site.

The results obtained are summarized in Table 5. The p -values were less than $\alpha = 0.05$ (statistical significance), i.e., for the two case studies, there was not enough evidence to reject the null hypothesis H_0 , concluding that the theoretical and real measurements do not have significant differences for the variables of thickness and length. In other words, it was statistically verified that, for crack thicknesses and lengths, the measurements obtained by the ImageJ software can be assimilated into the real measurements obtained in the field.

Table 5. Results of the Wilcoxon test for the theoretical and real crack/fissures measurements.

Sample	Size (n)	Significance (α)	p -Values	Result
Thickness	30	0.05	0.355	Not possible to reject H_0
Length	30	0.05	0.861	Not possible to reject H_0

5. Discussion

The results of the evaluation of cracks and fissures with the use of a UAV provided length and thickness parameters that are useful to describe the damage. In addition, the UAV technology used provided the tools for the bridge inspection, allowing access to hard-to-reach places. This practice would allow for reducing the traditional field inspections, leaving them only for specific cases.

By applying the evaluation techniques for images presented in this study, it was possible to obtain a descriptive damage identification about the dimensions and severity that would allow the specialist engineer to evaluate the damage remotely and make quick decisions, thus creating more agile and direct information management, and avoiding the field inspection to be prolonged.

Image analysis made it possible to reduce the number of images to be analyzed and to keep track of the damage found by using a low-cost UAV such as the DJI Mavic 2 model, which appropriately fulfilled the objective of recording cracks and fissures in the bridges.

In general, the use of UAV in bridge inspection provides a new vision of the structure without the need to be physically close to it, raising the need for new jobs for inspector-pilots that will require to be trained, where the procedure presented in this research could be part of such training. In summary, based on the experience gained by implementing the procedure presented in this research, Table 6 shows an analysis of the advantages and disadvantages of using UAVs for bridge inspection tasks.

Table 6. Advantages and disadvantages of using low-cost UAVs in bridge inspection.

Advantages	Disadvantages
It prevents the worker from having to expose himself to dangerous situations.	Regulatory standards limit the use of this equipment.
It has a direct reading for sample collection without a human presence on the inspected element.	For greater efficiency of image analysis, inspection tasks should be performed preferably during the day or with sufficient light.
A low-cost UAV can establish a precise flight path to access hard-to-reach places instead of using expensive aerial or sea/river platforms or other means of access.	It means a cost for the client due to the need to hire a specialized service or train his employees.
Environmentally friendly due to less pollution, avoiding the movement of heavy equipment and workers.	The battery life in low-cost UAVs is limited for inspecting large bridges, so extra batteries would be required, which increases costs.
It reduces inspection times on larger structures.	The inspection procedure is dependent on weather conditions, which must be favorable (e.g., low wind speed).
It reduces operating costs as no other accessibility methods are required, and a smaller number of workers are required.	The larger the audiovisual material collected, the larger the information to transfer and manage, which demands an appropriate management system.

Finally, it is important to note that although the present study did not consider other procedures to achieve greater precision in terms of orientation and georeferential information, such as the implementation of ground control points (GCP) in the drone flight areas, this would help minimize the problem of distortion of images. In fact, it could be considered to place permanent points for future inspections and reduce measuring costs. However, to reach the best possible image quality, the present study took advantage of the versatility of the drone used, positioning it in front of the element to be inspected orthogonally and, consequently, reducing perspective distortions significantly.

6. Conclusions

In this study, various image processing techniques were examined to detect cracks and fissures in bridges, using UAV as a tool to perform a visual inspection inventory. The technology used met expectations by reaching hard-to-reach areas where cracks are common. Additionally, it facilitated faster and greener inspections by minimizing environmental impact.

The images captured by the drone were suitable for analyzing cracks and fissures. The severity of the failures depends on the structural incidence and the thickness of the damage. The techniques evaluated for image processing were useful for improving visibility, although edge detection yielded mixed results. It was observed that this technique works best on individual cracks with regular bottoms, but in networks of cracks or failures in porous elements, the edges can become discontinuous.

Although traditional bridge inspection procedures will continue to be used, it is likely that in the near future, a fleet of UAV inspecting bridges can be implemented by government agencies or private companies, creating new jobs in the field and the office. This will require understanding and adapting inspection procedures such as the one presented in this study.

In terms of limitations, weather conditions (potential instability due to wind), battery life (large bridges demand longer times to inspect), and camera quality (edge detection becomes difficult when the image resolution is not high) are aspects to take into account when using low-cost UAVs. Another important aspect to consider is the possibility of working in difficult-to-access places where the drone cannot be perpendicularly positioned in front of the inspected element, which can cause perspective distortions in the captured image. Finally, based on the inspection procedure presented in this study, future research could consider using more sophisticated UAVs, increasing image quality and inspection times,

and dealing with unfavorable weather conditions, along with the use of photogrammetric processing to solve problems related to potential perspective distortions, while drones capture the images.

Author Contributions: Conceptualization, E.F., R.F.H. and J.S.-M.; methodology, O.R., H.S., R.F.H. and J.S.-M.; software, O.R. and H.S.; validation, E.F., R.F.H. and J.S.-M.; formal analysis, O.R., H.S. and J.S.-M.; investigation, E.F., O.R., H.S. and J.S.-M.; resources, E.F.; data curation, O.R. and H.S.; writing—original draft preparation, O.R. and H.S.; writing—review and editing, E.F., R.F.H. and J.S.-M.; visualization, O.R. and H.S.; supervision, E.F., R.F.H. and J.S.-M.; project administration, E.F. and J.S.-M.; funding acquisition, E.F. All authors have read and agreed to the published version of the manuscript.

Funding: This publication was supported by the Vice-Rector’s Office for Research and Doctorates of the Universidad San Sebastián, Chile—Fund number VRID_APC23/29.

Data Availability Statement: The data presented in this study are available on request from the corresponding author.

Acknowledgments: The authors would like to acknowledge the support provided by the following Chilean universities: Universidad San Sebastián, Universidad del Bío-Bío, and Pontificia Universidad Católica de Valparaíso.

Conflicts of Interest: The authors declare no conflicts of interest.

References

- Ruiz Esparza, G.; Callejo Silva, Ó.; Verdugo López, J. *Manual Para Conservación de Puentes y Estructuras Similares*, 1st ed.; Dirección General de Servicios Técnicos, Ed.; Secretaría de Comunicaciones y Transporte: Ciudad de México, Mexico, 2018.
- Feroz, S.; Abu Dabous, S. UAV-Based Remote Sensing Applications for Bridge Condition Assessment. *Remote Sens.* **2021**, *13*, 1809. [CrossRef]
- Peng, X.; Zhong, X.; Zhao, C.; Chen, A.; Zhang, T. A UAV-based machine vision method for bridge crack recognition and width quantification through hybrid feature learning. *Constr. Build. Mater.* **2021**, *299*, 123896. [CrossRef]
- Chilean Ministry of Public Works. *Volumen N°7—Manual de Carreteras “Mantenimiento Vial”*; Chilean Ministry of Public Works: Santiago, Chile, 2022; Volume 7.
- Valença, J.; Dias-da-Costa, D.; Júlio, E.; Araújo, H.; Costa, H. Automatic crack monitoring using photogrammetry and image processing. *Measurement* **2013**, *46*, 433–441. [CrossRef]
- Légeron, F.; Paultre, P.; Mazars, J. Damage Mechanics Modeling of Nonlinear Seismic Behavior of Concrete Structures. *J. Struct. Eng.* **2005**, *131*, 946–955. [CrossRef]
- Jeong, E.; Seo, J.; Wacker, J. Grayscale Drone Inspection Image Enhancement Framework for Advanced Bridge Defect Measurement. *Transp. Res. Rec. J. Transp. Res. Board* **2021**, *2675*, 603–612. [CrossRef]
- Forcael, E.; Ferrari, I.; Opazo-Vega, A.; Pulido-Arcas, J.A. Construction 4.0: A Literature Review. *Sustainability* **2020**, *12*, 9755. [CrossRef]
- Lattanzi, D.; Miller, G. Review of Robotic Infrastructure Inspection Systems. *J. Infrastruct. Syst.* **2017**, *23*, 1–16. [CrossRef]
- Kim, S.; Irizarry, J.; Costa, D.B. Field Test-Based UAS Operational Procedures and Considerations for Construction Safety Management: A Qualitative Exploratory Study. *Int. J. Civ. Eng.* **2020**, *18*, 919–933. [CrossRef]
- Ferreira, T.; Rasband, W. *The ImageJ User Guide*, 1st ed.; U.S. National Institutes of Health: Bethesda, MA, USA, 2012.
- Toirac Corral, J. Patología de la construcción: Grietas y fisuras en obras de hormigón; origen y prevención. *Cienc. Soc.* **2004**, *29*, 72–114. [CrossRef]
- Jeong, E.; Seo, J.; Wacker, J. Literature Review and Technical Survey on Bridge Inspection Using Unmanned Aerial Vehicles. *J. Perform. Constr. Facil.* **2020**, *34*, 04020113. [CrossRef]
- Seo, J.; Wacker, J.P.; Duque, L. *Evaluating the Use of Drones for Timber Bridge Inspection*; U.S. Department of Agriculture, Forest Service, Forest Products Laboratory: Madison, WI, USA, 2018.
- Ng, R.; Levoy, M.; Brédif, M.; Duval, G.; Horowitz, M.; Hanrahan, P. *Light Field Photography with a Hand-Held Plenoptic Camera*; Stanford Computer Graphics Laboratory: Palo Alto, CA, USA, 2005.
- Pereira, J. Digital Heritage. Available online: <http://www.jpereira.net/gestion-de-color-articles/mediciones-y-asignacion-de-escala-en-fotografias> (accessed on 1 October 2023).
- Vincent, O.; Folorunso, O. A Descriptive Algorithm for Sobel Image Edge Detection. In Proceedings of the Informing Science & IT Education Conference (InSITE), Macon, CA, USA, 12–15 June 2009; Volume 40, pp. 97–107.
- Parker, J.R. *Algorithms for Image Processing and Computer Vision*, 2nd ed.; Wiley: Indianapolis, IN, USA, 2010; ISBN 978-0-470-64385-3.
- Kheradmand, A.; Milanfar, P. A General Framework for Regularized, Similarity-Based Image Restoration. *IEEE Trans. Image Process.* **2014**, *23*, 5136–5151. [CrossRef] [PubMed]

20. Rashmi; Kumar, M.; Saxena, R. Algorithm and Technique on Various Edge Detection: A Survey. *Signal Image Process. Int. J.* **2013**, *4*, 65–75. [[CrossRef](#)]
21. Lei, B.; Wang, N.; Xu, P.; Song, G. New Crack Detection Method for Bridge Inspection Using UAV Incorporating Image Processing. *J. Aerosp. Eng.* **2018**, *31*, 1–13. [[CrossRef](#)]
22. Sarkar, K.; Shiuly, A.; Dhal, K.G. Revolutionizing concrete analysis: An in-depth survey of AI-powered insights with image-centric approaches on comprehensive quality control, advanced crack detection and concrete property exploration. *Constr. Build. Mater.* **2024**, *411*, 134212. [[CrossRef](#)]
23. Basalamah, A. An Interactive Tool for Teaching the Central Limit Theorem to Engineering Students. *Int. J. Adv. Comput. Sci. Appl.* **2021**, *12*, 813–817. [[CrossRef](#)]
24. Shapiro, S.S.; Wilk, M.B. An Analysis of Variance Test for Normality (Complete Samples). *Biometrika* **1965**, *52*, 591–611. [[CrossRef](#)]
25. Khatun, N. Applications of Normality Test in Statistical Analysis. *Open J. Stat.* **2021**, *11*, 113–122. [[CrossRef](#)]
26. Sultan, A.A.; Mashrei, M.A.; Washer, G.A. Utilization of Wilcoxon-Mann-Whitney statistics in assessing the reliability of nondestructive evaluation technologies. *Structures* **2020**, *27*, 780–787. [[CrossRef](#)]

Disclaimer/Publisher’s Note: The statements, opinions and data contained in all publications are solely those of the individual author(s) and contributor(s) and not of MDPI and/or the editor(s). MDPI and/or the editor(s) disclaim responsibility for any injury to people or property resulting from any ideas, methods, instructions or products referred to in the content.